Electronic Supplementary Material (ESI) for Journal of Materials Chemistry A.

Electronic Supplemental Information for *Phase Transformations and Capacity Fade Mechanism in Li_xSn Nanoparticle Electrodes Revealed by Operando ^7Li NMR*

Jose L. Lorie Lopez, Philip J. Grandinetti, Anne C. Co
Department of Chemistry and Biochemistry, The Ohio State University,
100 West 18th Ave. Columbus OH, 43210-1340, USA

Li Site	x	x_{Sn}	δ/ppm	T_1/s
Li_2Sn_5	0.4	0.7143	78	0.98 ± 0.05
LiSn	1.0	0.50	42	1.98 ± 0.04
LiSn	1.0	0.50	32	1.87 ± 0.01
Li_7Sn_3	$2.\overline{3}$	0.30	17.5	2.63 ± 0.30
Li_5Sn_2	2.5	0.286	14.3	2.63 ± 0.30
$Li_{13}Sn_5$	$2.\overline{6}$	0.278	16.7	2.63 ± 0.30
Li_7Sn_2	3.5	0.222	9.5	-
$Li_{7-\zeta}Sn_3$	1.8	0.30	$\sim$15	1.83 ± 0.03

Table S1: ^{7}Li magnetization longitudinal relaxation times and shifts determined in-situ in a Li-Sn cell during the lithiation/delithiation of the first cycle. All shift values of Li-Sn intermetallic phases were reported by Bekaert et al. [1] except for $Li_{7-\zeta}Sn_3$.

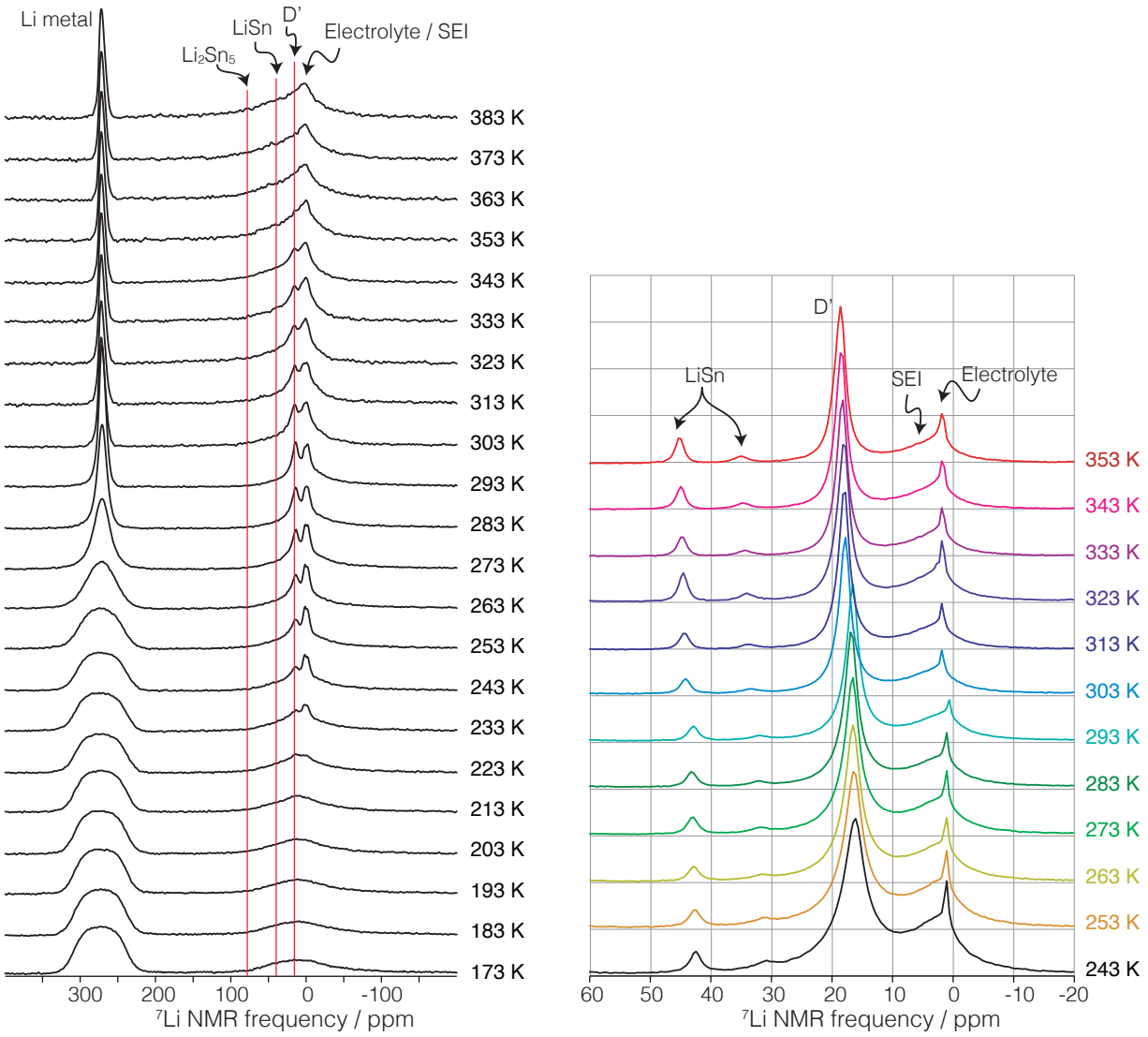

Figure S1: (A) In-situ variable temperature ^{7}Li static NMR spectra of a Sn electrode lithiated to $Li_{7-\zeta}Sn_3$. Spectra were obtained using an rf power of 150 W. A 5 μs pulse length was used giving a tip angle of 36 ° for the intermetallics and electrolyte, and 72 ° for the Li metal. A recycle delay of 0.65 s was used and 440 scans were averaged together for each spectrum. (B) Ex-situ variable temperature ^{7}Li MAS NMR spectra of the $Li_{7-\zeta}Sn_3$. Spectra were acquired with a Bruker 4 mm MAS probe at a spinning speed of 12 kHz and a $\pi/2$ pulse length of a 4 μs at 50 W, with 8 scans. A 45 s recycle delay was used for measurements between 243 K and 283K, a 30 s recycle delay for measurements between 293 K and 333K, and a 20 s delay for the measurements at 343 K and 353 K.

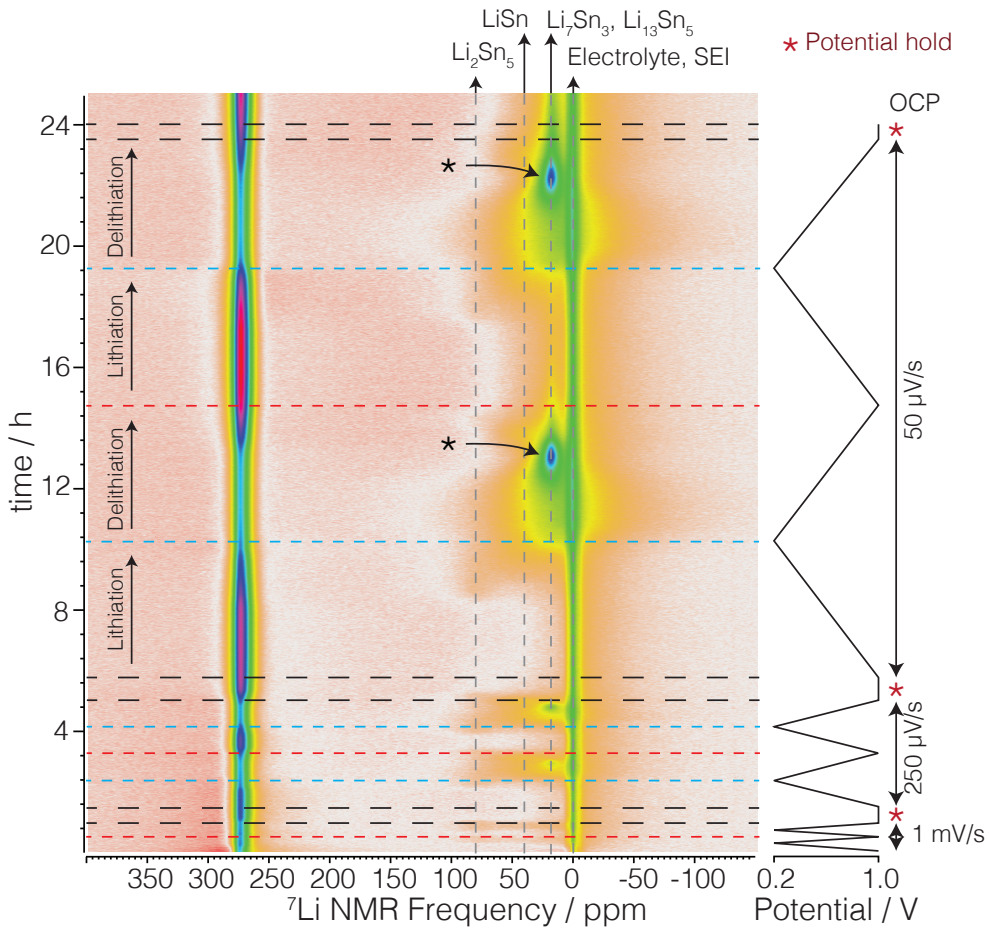

Figure S2: The effect of sweep rates on the lithiation and delithiation of Sn electrodes was examined with operando ^{7}Li NMR 2D spectra of a Sn electrode at 1000, 250, and 50 μV/s. Thirty minutes of potential hold at 1.0 V was conducted between each cycling regimes. During the first two cycles at 1000 μV/s only small signals of Li_2Sn_5 and LiSn are present even though the potential is swept to 0.2 V. This is consistent with previous observations that only the electrode surface is involved in the electrochemical Li process, particularly at relatively fast scan rates [2]. The next two cycles at 250 μV/s show characteristics of the formation of the Li_7Sn_3 group at 17.5 ppm and Li_7Sn_2 at 9.5 ppm. As the scan rate is decreased to 50 μV/s, the amount of lithiated Sn increases, where the formation of Li_7Sn_3 and Li_7Sn_2 is clearly present. During delithiation, the $Li_{7-\zeta}Sn_3$ phase also appears and becomes more intense during subsequent cycles.

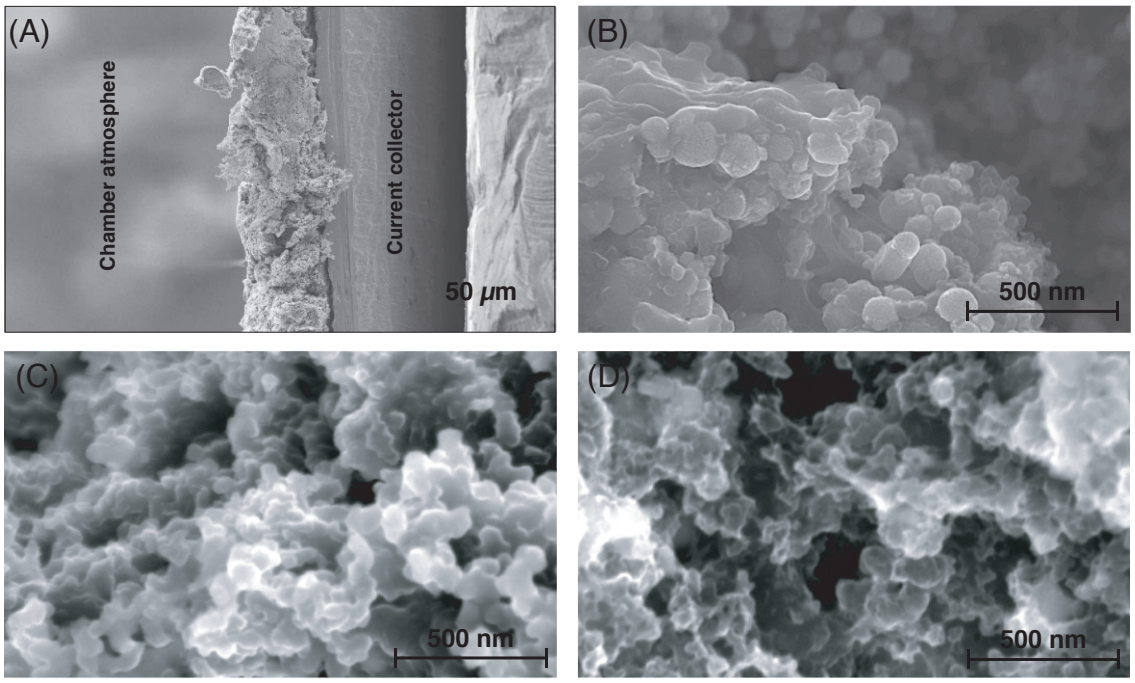

Figure S3: A FEI/Philips Sirion Field Emission scanning electron microscope (SEM) was used to probe the electrode surface morphology, as well as the uniformity of the electrode's thickness and the micrographs. In (A) is the SEM showing the thickness of the as-prepared electrode. In (B) is the SEM image of a fresh electrode, in (C) is the SEM image of the electrode cycled to Li_7Sn_3, and in (D) is the SEM image of the electrode cycled to the vacancy rich $Li_{7-\zeta}Sn_3$. When casted into an electrode film, the Sn nanoparticles maintained their 60-80 nm size, resulting in nanoporous features in the same order of magnitude. The Sn nanoparticle film is relatively uniform when casted giving an electrode thickness in the range of 30 - 40 μm. Once dried, the film contained macrochannels in the order of 150 - 200 μm.

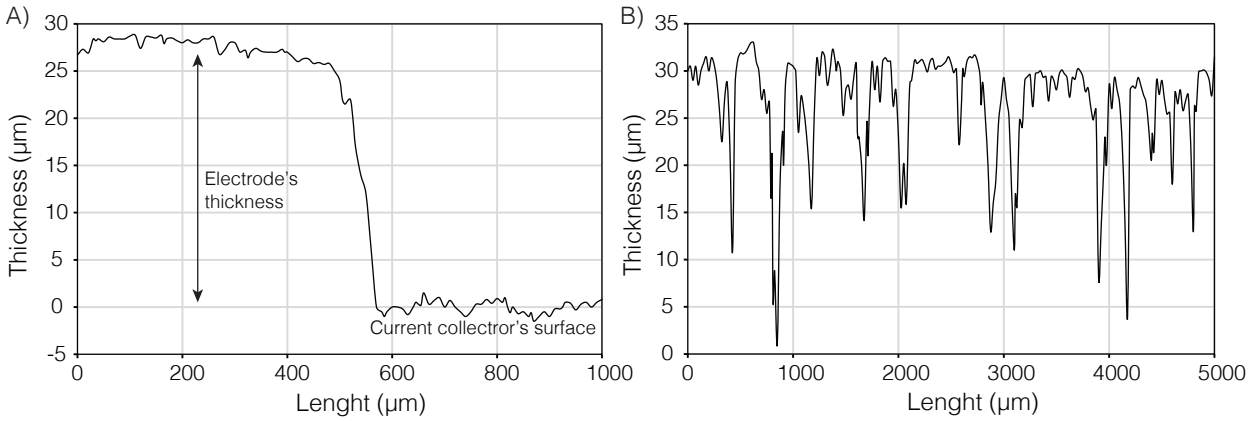

Figure S4: Surface profile of a fresh electrode showing in (A) that the electrode thickness measured as of $\sim$30 μm against the copper current collector surface and in (B) that the macroporous channels present in the electrode are between 150 to 250 μm wide. The electrode thickness was also measured using an Alpha-Step® 500 Surface Profiler with a stylus force of 25.9 mg and a scan rate of 50 μm/s.

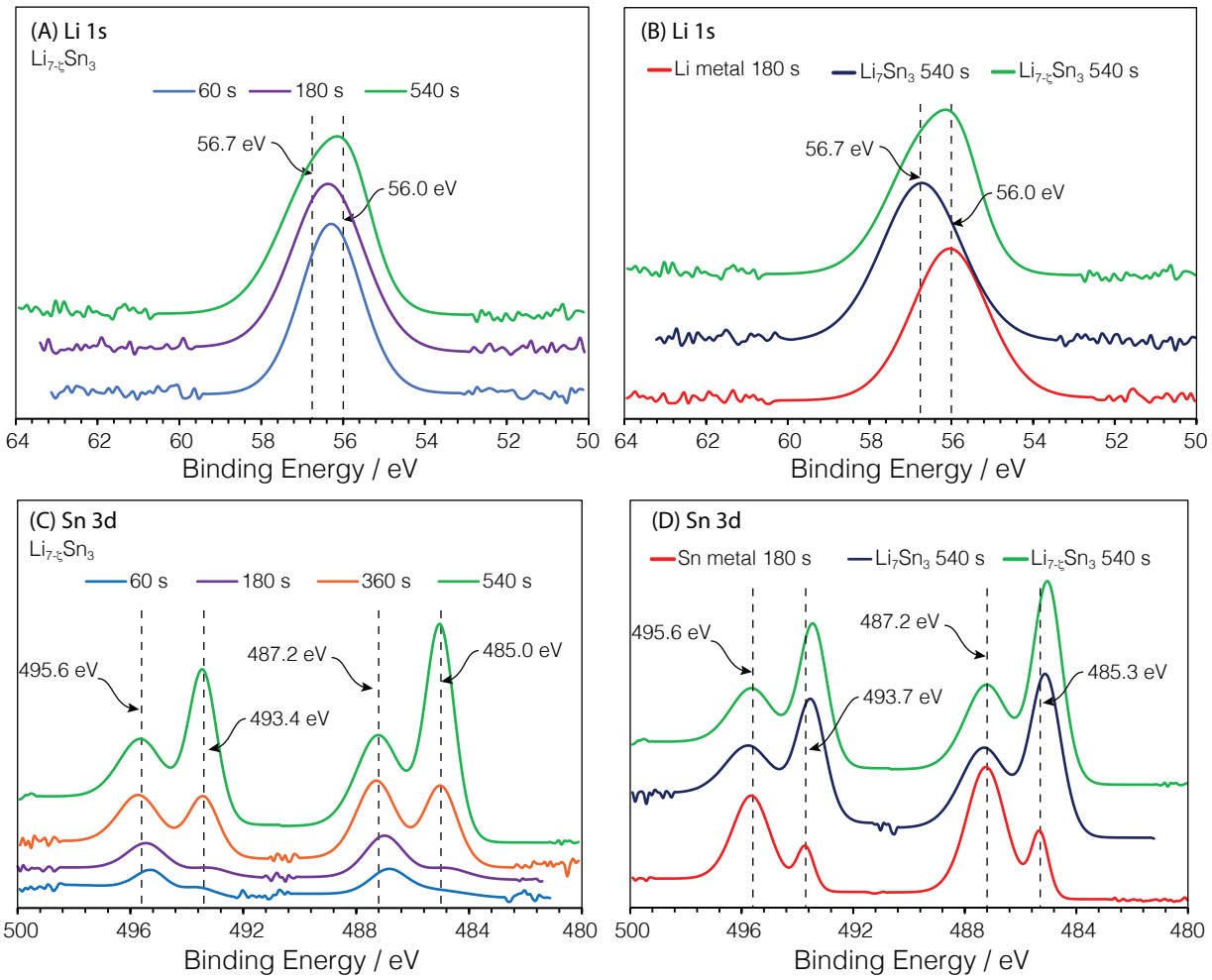

Figure S5: X-ray photoelectron microscopy was used to analyze any changes in the oxidation states of the lithium and tin in two samples, Li_7Sn_3 formed during lithiation, and the vacancy rich $Li_{7-\zeta}Sn_3$ formed during delithiation. In this figure are the X-ray photoelectron spectra of Li_7Sn_3 and $Li_{7-\zeta}Sn_3$ obtained during lithiation and delithiation, respectively. In (A) is the Li 1s spectra of the $Li_{7-\zeta}Sn_3$ as a function of etching time. In (B) is the Li 1s comparison of the $Li_{7-\zeta}Sn_3$ and Li_7Sn_3 to Li metal. In (C) is the Sn 3d spectra of the $Li_{7-\zeta}Sn_3$ as a function of etching time. In (D) is the Sn 3d comparison of the $Li_{7-\zeta}Sn_3$ and Li_7Sn_3 to Sn metal. The Li 1s shows a shift and peak broadening while the Sn 3d shows the emergence of the metallic Sn peaks at 485.0 and 493.4 eV for the Sn 3/2 and 5/2, respectively. The SnO_2 peaks at 487.2 and 495.6 eV, however, show minor changes in intensity as the electrode is composed of nanoparticles and their surface is always being probed. Comparing the peaks of the $Li_{7-\zeta}Sn_3$ to those of the reference metal and Li_7Sn_3, the Li 1s in (B) reveals a shift of 0.7 eV for Li_7Sn_3 with respect to the lithium metal. The $Li_{7-\zeta}Sn_3$ on the other hand, exhibits a broad peak with contributions from both the Li metal and the standard Li_7Sn_3. The Sn 3d result indicates that the Sn 3/2 peak at 485.3 eV for both Li_7Sn_3 and $Li_{7-\zeta}Sn_3$ are shifted 0.3 eV from that of metallic Sn, indicating that the oxidation states of Li and Sn in Li_7Sn_3 and $Li_{7-\zeta}Sn_3$ are very similar and that their structures are related.

References

[1] Emilie Bekaert, F. Robert, P.E. Lippens, and M.Ménétrier. ^{7}Li NMR Knight shifts in Li-Sn compounds: MAS NMR measurements and correlation with DFT calculations. *J. Phys. Chem. C*, 114:6749–6754, 2010.

[2] D. X. Liu, J. Wang, K. Pan, J. Qiu, M. Canova, L. R. Cao, and A. C. Co. In situ quantification and visualization of lithium transport with neutrons. *Angew. Chem. Int. Edit.*, 53:9498 – 9502, 2014.